1^{-+} hybrid meson in J/ψ radiative decays from lattice QCD

Feiyu Chen,[1,2,*] Xiangyu Jiang,[1,2,†] Ying Chen,[1,2,‡] Ming Gong,[1,2] Zhaofeng Liu,[1,2,3] Chunjiang Shi,[1,2] and Wei Sun[1]

[1]*Institute of High Energy Physics, Chinese Academy of Sciences, Beijing 100049, People's Republic of China*

[2]*School of Physics, University of Chinese Academy of Sciences, Beijing 100049, People's Republic of China*

[3]*Center for High Energy Physics, Peking University, Beijing 100871, People's Republic of China*

(Received 21 July 2022; accepted 16 March 2023; published 28 March 2023)

We present the first theoretical prediction of the partial decay width of the process $J/\psi \to \gamma\eta_1$, where η_1 is the lightest flavor singlet 1^{-+} hybrid meson. Our $N_f = 2$ lattice QCD calculation at $m_\pi \approx 350$ MeV results in the η_1 mass $m_{\eta_1} = 2.23(4)$ GeV and the related electromagnetic form factors $M_1(0) = -4.73(74)$ MeV, $E_2(0) = 1.18(22)$ MeV, which give $\Gamma(J/\psi \to \gamma\eta_1) = 2.04(61)$ eV. These form factors can be applied to the physical $N_f = 3$ case, where there should be two hybrid mass eigenstates $\eta_1^{(l)}$ and $\eta_1^{(h)}$ due to the singlet-octet mixing. It is shown that the ratio of the branching fractions $\mathrm{Br}(J/\psi \to \gamma\eta_1^{(l,h)} \to \gamma\eta\eta')$ is inversely proportional to the ratio of the total widths of $\eta_1^{(l,h)}$. Given our results and the mixing angle derived by a previous lattice study, whether $\eta_1(1855)$ is assigned to be $\eta_1^{(1)}$ or $\eta_1^{(h)}$, the observed branching fraction $J/\psi \to \eta_1(1855) \to \gamma\eta\eta'$ implies a very large coupling of the octet η_1 to $\eta\eta'$. This should be investigated in future studies.

DOI: 10.1103/PhysRevD.107.054511

I. INTRODUCTION

Gluons and quarks are fundamental degrees of freedom of quantum chromodynamics (QCD). It is expected that gluons can also serve as building blocks to form hadrons. In the quark model picture, the hadrons made up of valence quarks and valence gluons are usually called hybrids. The hybrid mesons with $J^{PC} = 1^{-+}$ are most intriguing since this quantum number is prohibited for $q\bar{q}$ states of quark model. Up to now, there are three experimental candidates for $I^G J^{PC} = 1^- 1^{-+}$ light hybrid mesons, namely, $\pi_1(1400)$ [1], $\pi_1(1600)$ [2–4], and $\pi_1(2105)$ [2] (details can be found in the latest review [5] and the references therein), while lattice QCD studies [6–13] predict that the mass of isovector 1^{-+} hybrid meson has a mass around 1.7–2.2 GeV for light quark masses in a range up to the strange quark mass. Very recently, the BESIII Collaboration reported the first observation of a $I^G J^{PC} = 0^+ 1^{-+}$ structure $\eta_1(1855)$ through the partial wave analysis of the $J/\psi \to \gamma\eta\eta'$ process [14,15]. The resonance parameters of $\eta_1(1855)$ are determined to be $m_{\eta_1} = 1855 \pm 9^{+6}_{-1}$ MeV and $\Gamma_{\eta_1} = 188 \pm 18^{+3}_{-8}$ MeV, and the branching fraction $\mathrm{Br}(J/\psi \to \gamma\eta_1(1855) \to \gamma\eta\eta')$ is $(2.70 \pm 0.41^{+0.16}_{-0.35}) \times 10^{-6}$. There have been several phenomenological studies on the properties of $\eta_1(1855)$ by assuming it to be an isoscalar light hybrid [16–18], a $K\bar{K}_1(1400)$ molecular state [19,20], or a tetraquark state [21,22]. As far as the hybrid assignment is concerned, there should be two isoscalar 1^{-+} mesons in the flavor SU(3) nonet, and a $N_f = 2 + 1$ lattice QCD study [12] does observe two states of masses around 2.16 GeV and 2.33 GeV, respectively, in the $0^+ 1^{-+}$ channel (note the light quark mass here corresponds to a pion mass $m_\pi \sim 390$ MeV). It is noticed that BESIII also reports a 1^{-+} state around 2.2 GeV in the same channel with statistical significance 4.4σ [15].

Since $\eta_1(1855)$ is observed in the J/ψ radiative decay, with regard to the possible hybrid assignment, it is desirable to know the production property of the 1^{-+} hybrid meson (named as η_1 also) in this process, which will provide important information to the nature of $\eta_1(1855)$. This can be investigated in the lattice QCD formalism through the approach similar to the cases of $q\bar{q}$ mesons [23] and glueballs [24–26] in J/ψ radiative decays. The key task

*chenfy@ihep.ac.cn
†jiangxiangyu@ihep.ac.cn
‡cheny@ihep.ac.cn

TABLE I. Parameters of the gauge ensemble.

$L^3 \times T$	β	a_t^{-1} (GeV)	ξ	m_π (MeV)	$N_{\rm cfg}$
$16^3 \times 128$	2.0	6.894(51)	~5.3	348.5(1.0)	6991

is to extract the related electromagnetic multipole form factors from the corresponding three-point functions with a vector current insertion, which involve obviously the annihilation diagrams of the light u, d quarks. Therefore, we adopt the distillation method [27] in the practical calculation, which provides a sophisticated scheme for the operator construction and the computation of all-to-all quark propagators.

This paper is organized as follows: Section II presents the details of the numerical calculations of three-point functions, the extraction of the form factors, and the interpolation of the form factors to on shell ones. The discussion of the phenomenological implications of our results can be found in Sec. III. Section IV is a brief summary.

II. NUMERICAL DETAILS

A large statistics is mandatory for the study of J/ψ radiative decay into light hadrons. Our gauge ensemble of $N_f = 2$ degenerate u, d quarks includes 6991 gauge configurations, which are generated on an $L^3 \times T = 16^3 \times 128$ anisotropic lattice with the anisotropy parameter $\xi = a_s/a_t = 5.3$ (a_s and a_t are the spatial and temporal lattice spacing, respectively) [28]. The sea quark mass is tuned to give the pion mass $m_\pi \approx 350$ MeV. The parameters of the gauge ensemble are collected in Table I. For the valence charm quark, we adopt the clover fermion action in Ref. [29], and the charm quark mass parameter is set by $(m_{\eta_c} + 3m_{J/\psi})/4 = 3069$ MeV. For each source time slice $\tau \in [0, T-1]$ on each gauge configuration, the perambulators of light u, d quarks are calculated in the Laplacian Heaviside subspace spanned by $N_{\rm vec} = 70$ eigenvectors with lowest eigenvalues.

A. Three-point functions

The partial decay width of $J/\psi \to \gamma\eta_1$ is governed by the on shell electromagnetic form factors $M_1(Q^2 = 0)$ and $E_2(Q^2 = 0)$ ($Q^2 = -p_\gamma^2$), namely,

$$\Gamma(J/\psi \to \gamma\eta_1) = \frac{4\alpha}{27}\frac{|\vec{p}_\gamma|}{m_{J/\psi}^2}(|M_1(0)|^2 + |E_2(0)|^2), \quad (1)$$

where $\alpha = 1/134$ is the fine structure constant at the charm quark mass scale and $\vec{p}_\gamma$ is the momentum of the final state photon with $|\vec{p}_\gamma| = (m_{J/\psi}^2 - m_{\eta_1}^2)/(2m_{J/\psi})$ in the rest frame of J/ψ. These on shell form factors can be obtained by the $Q^2 \to 0$ interpolation or extrapolation of the form factors $M_1(Q^2)$ and $E_2(Q^2)$, which are defined through the multipole decomposition of the transition matrix elements $\langle\eta_1(p',\lambda')|j^\mu_{\rm em}(0)|J/\psi(p,\lambda)\rangle$ (see the Appendix and also Refs. [30,31]). These matrix elements can be extracted from the following three-point functions:

$$\Gamma^{(3)}_{i\mu j}(\vec{p},\vec{p}',t,t') = \sum_{\vec{x}} e^{-i\vec{q}\cdot\vec{x}}\langle\Omega|T\mathcal{O}^i_{\eta_1}(\vec{p}',t)j^\mu_{\rm em}(\vec{x},t') \times \mathcal{O}^{j\dagger}_{J/\psi}(\vec{p},0)|\Omega\rangle, \quad (2)$$

where $j^\mu_{\rm em}$ is the electromagnetic current of quarks, and $\mathcal{O}^i_{\eta_1}(\vec{p},t)$ and $\mathcal{O}^j_{J/\psi}(\vec{p},t)$ are the interpolation operators generating η_1 and J/ψ states with a spatial momentum $\vec{p}$. Therefore, the major numerical task is to calculate these three-point functions from lattice QCD.

Our lattice setup has the exact SU(2) isospin symmetry. The lattice operator for the isoscalar η_1 takes the form $\mathcal{O}^i_{\eta_1} = \frac{1}{\sqrt{2}}\epsilon^{ijk}(\bar{u}\gamma_j B_k u + \bar{d}\gamma_j B_k d)$, where the chromomagnetic field strength B_k is constructed by the proper combination of the gauge covariant spatial derivatives on the lattice [12]. For the operator $\mathcal{O}^i_{J/\psi}$, we use the conventional $\bar{c}\gamma^i c$-type operator. In order to avoid the complication that the momentum projected operator $\mathcal{O}^i_{\eta_1}$ can couple to states with quantum numbers other than 1^{-+} [32], the three-point functions in Eq. (2) are calculated practically in the rest frame of η_1 with J/ψ moving at different spatial momenta $\vec{p}$. It has been tested that the dispersion relation of J/ψ satisfies the continuum form very well for all the $\vec{p}$ modes involved [28].

We only consider the initial state radiation and ignore the case that the photon is emitted from quarks in the final state, so the electromagnetic current $j^\mu_{\rm em}$ involves charm quarks, namely, $j^\mu_{\rm em} = Z_V\bar{c}\gamma^\mu c$ [the electric charge of the charm quark $Q_c = \frac{2}{3}e$ has been absorbed in the prefactor in Eq. (1)]. Here, Z_V is the renormalization constant of the current, since $j^\mu_{\rm em}$ is not a conserved vector current operator on the lattice. In practice, only the spatial components of $j^\mu_{\rm em}$ is involved, and its renormalization constant $Z_V^s = 1.118(4)$ [23] is incorporated implicitly into the expressions in the rest part of this work.

Figure 1 illustrates the schematic diagram of $\Gamma^{(3)}_{i\mu j}$ after Wick's contraction. It has two separated quark loops, which are actually connected by gluons. The light quark loop on the right-hand side can be calculated in the framework of the distillation method. The left part comes from the product of $\mathcal{O}_{J/\psi}$ and the current $j^\mu_{\rm em}$, namely,

$$G_{\mu i}(\vec{p},\vec{q};t'+\tau,\tau) = \sum_{\vec{x}} e^{-i\vec{q}\cdot\vec{x}} j^\mu_{\rm em}(\vec{x},t'+\tau)O^{i\dagger}_{J/\psi}(\vec{p},\tau), \quad (3)$$

which looks very similar to a conventional two-point function of J/ψ and can be calculated independently on each gauge configuration. However, in order for $\Gamma^{(3)}_{i\mu j}$ to

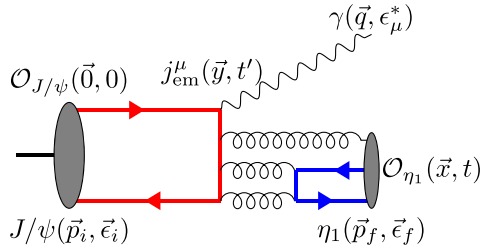

FIG. 1. The schematic diagram of the process $J/\psi \to \gamma\eta_1$.

have good enough signals, the calculation of $G_{\mu i}$ is highly nontrivial. The conventional momentum source technique turns out to be unfeasible here, because the resulted three-point functions,

$$\Gamma^{(3)}_{i\mu j}(\vec{p},\vec{0};t,t') = \frac{1}{T}\sum_{\tau=0}^{T-1}\langle \mathcal{O}^i_{\eta_1}(\vec{0},t+\tau)G_{\mu j}(\vec{p},\vec{p};t'+\tau,\tau)\rangle, \tag{4}$$

are too noisy even though we have a large gauge ensemble and average over all the time slices τ.

In order to circumvent this difficulty, we calculate $G_{\mu i}$ in the framework of the distillation method. The distillation method provides a gauge covariant smearing scheme for quark fields, taking the charm quark field $c(x)$, for instance, $c^{(s)}(\vec{x},t) = \sum_{\vec{y}}[VV^\dagger(t)](\vec{x},\vec{y})c(\vec{y},t)$, where $V(t)$ is the matrix whose columns are eigenvectors of the lattice Laplacian operator $-\nabla^2(t)$ at t (we use $N^{(c)}_{\rm vec} = 50$ vectors for charm quarks). Therefore, we use the operator $\mathcal{O}^i_{J/\psi}(\vec{p},t) = \sum_{\vec{y}} e^{-i\vec{p}\cdot\vec{y}}[\bar{c}^{(s)}\gamma_i c^{(s)}](\vec{y},t)$ to calculate $G_{\mu i}$, whose explicit expression for source time slice at $\tau = 0$ is

$$G_{\mu i}(\vec{p},\vec{q};t,0) = \sum_{\vec{x}} e^{-i\vec{q}\cdot\vec{x}}\mathrm{Tr}\,\{\gamma_5[S_c V(0)]^\dagger(\vec{x},t)\gamma_5\gamma^\mu \times [S_c V(0)](\vec{x},t)[V^\dagger(0)D(\vec{p})\gamma_i V(0)]\}, \tag{5}$$

where $S_c = \langle c\bar{c}\rangle_U$ is the all-to-all propagator of charm quark for the gauge configuration U and $D(\vec{p})$ is a $3L^3 \times 3L^3$ diagonal matrix with the diagonal matrix elements being $\delta_{ij}e^{i\vec{p}\cdot\vec{y}}$ ($\vec{y}$ labels the column or row indices and i, $j = 1,2,3$ refer to the color indices). Here, we apply the γ_5-Hermiticity of S_c, namely, $S_c = \gamma_5 S_c^\dagger \gamma_5$, which implies $[V^\dagger(0)S_c](\vec{x},t) = \gamma_5[S_c V(0)]^\dagger(\vec{x},t)\gamma_5$, such that what we actually calculate is $S_c V(0)$ by solving the linear equation arrays,

$$M[U;m_c][S_c V(0)] = V(0), \tag{6}$$

where $M[U;m_c]$ is the fermion matrix in the lattice action of the charm quark. At the source time slice $\tau = 0$, we have to solve the linear equation defined by $M[U;m_c]$ for each Dirac index $\alpha = 1,2,3,4$ and each column of $V(0)$. In practice, we repeat the above procedure by letting the source time slice τ running over all the time range, say, $\tau \in [0, T-1]$, to increase the statistics further. This procedure requires 25,600 inversions of $M[U;m_c]$ on each gauge configuration, apart from the calculation of the perambulators of u, d quarks. This prescription turns out to be crucial for us to obtain good signals of the three point functions, from which we can extract the multipole form factors with an acceptable precision.

B. Extraction of form factors

When $t \gg t' \gg 0$, the three-point function $\Gamma^{(3)}_{i\mu j}(\vec{p},\vec{0};t,t')$ can be parametrized as

$$\Gamma^{(3)}_{i\mu j}(\vec{p},\vec{0};t,t') \approx \frac{Z_{\eta_1}(\vec{0})Z^*_{J/\psi}(\vec{p})}{4m_{\eta_1}E_{J/\psi}(\vec{p})}e^{-m_{\eta_1}(t-t')}e^{-E_{J/\psi}(\vec{p})t'} \times \mathcal{M}^{i\mu j}(\vec{p}), \tag{7}$$

where $Z_{\eta_1}(\vec{0})$ and $Z_{J/\psi}(\vec{p})$ come from the matrix element $\langle\Omega|\mathcal{O}^i_X|X(\vec{p},\lambda)\rangle = Z_X(\vec{p})\epsilon^i_\lambda(\vec{p})$ with X referring J/ψ or η_1 and $\epsilon^\mu_\lambda(\vec{p})$ being its λth polarization vector [note that $Z_X(\vec{p})$ depends on $|\vec{q}|$ since $\mathcal{O}_X(\vec{p})$ is a smeared operator [33]], and $\mathcal{M}^{i\mu j}(\vec{p})$ is the desired matrix element at $\vec{p}$,

$$\mathcal{M}^{i\mu j}(\vec{p}) = \sum_{\lambda,\lambda'}\epsilon^i_{\lambda'}(\vec{0})\langle\eta_1(\vec{0},\lambda')|j^\mu_{\rm em}(0)|J/\psi(\vec{q},\lambda)\rangle\epsilon^{*j}_\lambda(\vec{p}), \tag{8}$$

which is encoded with the multipole form factors $M_1(Q^2)$, $E_2(Q^2)$ etc.

Obviously, in order to extract $\mathcal{M}^{i\mu j}(\vec{p})$, we should know the parameters $Z_X(\vec{p})$, m_{η_1}, and $E_{J/\psi}(\vec{p})$, which are actually included in the two-point functions of η_1 and J/ψ, namely,

$$\Gamma^{(2)}_X(\vec{p},t) = \frac{1}{3T}\sum_{\tau=0}^{T-1}\sum_{i=1}^{3}\langle\mathcal{O}_{X,i}(\vec{p},\tau+t)\mathcal{O}^\dagger_{X,i}(\vec{p},\tau)\rangle = \left(1+\frac{|\vec{p}|^2}{3m_X^2}\right)\sum_n\frac{|Z^{(n)}_X(\vec{p})|^2}{2E^{(n)}_X(\vec{p})}e^{-E^{(n)}_X(\vec{p})t}, \tag{9}$$

where X stands for J/ψ or η_1 and the source time slice τ is averaged to increase the statistics. The operators $\mathcal{O}_X$ must be the same as those in the three-point functions $\Gamma^{(3)}_{i\mu j}$; therefore, $\Gamma^{(2)}_X(\vec{p},t)$'s are calculated with the distillation method as well. Since η_1 is set to be at rest, we only calculate $\Gamma^{(2)}_{\eta_1}(\vec{p},t)$ at $\vec{p} = 0$. The effective mass plot is shown in Fig. 2, where the effective mass of the isovector 1^{-+} hybrid state (usually named π_1) is also plotted for comparison. The effective mass of η_1 has a much worse signal than that of π_1 due to the inclusion of disconnected diagrams. Through two-mass-term fits in the time range $t \in [4,14]$ for η_1 and $t \in [10,30]$ for π_1, the masses are

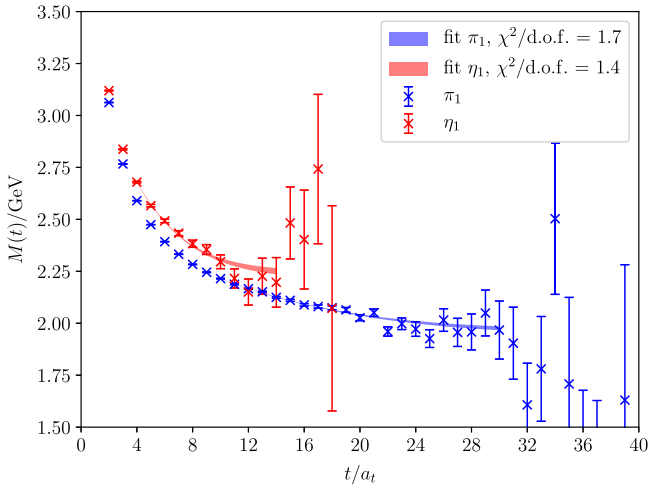

FIG. 2. Effective mass of π_1 (isovector) and η_1 (isoscalar), where the fit ranges are [10, 30] and [4, 14], respectively. The shaded curves illustrate the best-fit values with errors using two-mass-term fits.

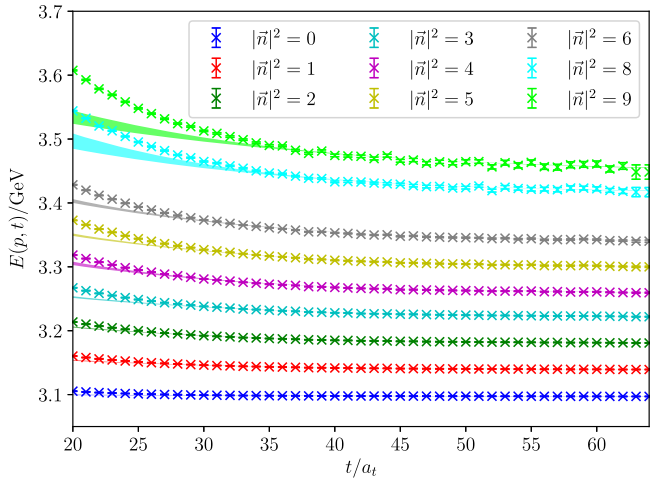

FIG. 3. The effective energies of J/ψ at different spatial modes with $|\vec{n}|^2 \leq 9$. The data points are the numerical results from $\Gamma^{(2)}_{J/\psi}(\vec{p},t)$, and the shaded curves illustrate the best-fit values with errors.

determined to be $m_{\pi_1} = 1.950(28)$ GeV and $m_{\eta_1} = 2.230(39)$ GeV, respectively. These results are consistent with those in Ref. [12].

In order for Q^2 to cover the range around $Q^2 = 0$, the spatial momentum $\vec{p} = \frac{2\pi}{La_s}\vec{n}$ of J/ψ is set to run through all possible modes with $|\vec{n}|^2 \leq 9$ based on the m_{η_1} obtained above. Since $\mathcal{O}_{J/\psi}(\vec{p},t)$ involved in $\Gamma^{(3)}_{i\mu j}$ is a smeared operator with $N^{(c)}_{\text{vec}} = 50$, we also generate the perambulators of the valence charm quark with the same $N^{(c)}_{\text{vec}}$ to calculate $\Gamma^{(2)}_{J/\psi}(\vec{p},t)$. The energies $E_{J/\psi}(\vec{p}) \equiv E^{(0)}_{J/\psi}(\vec{p})$ of J/ψ for all the momentum modes involved can be precisely extracted from $\Gamma^{(2)}_{J/\psi}(\vec{p},t)$ through two-mass-term fits. Figure 3 shows the effective energies $E(\vec{p},t)$ (data points) and the fits (colored bands) at different momentum modes $\vec{n}$ up to $|\vec{n}|^2 = 9$.

Along with the calculated two-point functions of J/ψ and η_1, the matrix element $\mathcal{M}^{i\mu j}(\vec{p})$ is extracted from the ratio function,

$$\mathcal{M}^{i\mu j}(\vec{p},t,t') = \frac{\left(1+\frac{|\vec{p}|^2}{3m^2_{J/\psi}}\right) Z_{J/\psi}(\vec{p}) Z_{\eta_1} \Gamma^{(3)}_{i\mu j}(\vec{p},\vec{0};t,t')}{\Gamma^{(2)}_{\eta_1}(\vec{0},t-t')\Gamma^{(2)}_{J/\psi}(\vec{p},t')}, \tag{10}$$

which suppresses the contamination from higher states and should be independent of t and t' when ground states dominate. We then make a weighted average value of the function on t' to get larger statistics, and take a convention $\Delta t = t - t'$,

$$\mathcal{M}^{i\mu j}(\vec{p},\Delta t) = \frac{\sum_{t'=20}^{40}\left(\frac{1}{\Delta^{i\mu j}_{\mathcal{M}}}\right)^2 \mathcal{M}^{i\mu j}(\vec{p},t'+\Delta t,t')}{\sum_{t'=20}^{40}\left(\frac{1}{\Delta^{i\mu j}_{\mathcal{M}}}\right)^2}, \tag{11}$$

where $\Delta^{i\mu j}_{\mathcal{M}}$ is the error of the corresponding ratio function, and the weight is $(\frac{1}{\Delta^{i\mu j}_{\mathcal{M}}})^2$ to make the average value equal to the least square fit result using a constant. $t' \in [20,40]$ indicates the "fitting window" in this step. Subsequently, We can extract the form factors $M_1(Q^2,\Delta t)$ and $E_2(Q^2,\Delta t)$ from the linear combination of matrix elements $\mathcal{M}^{i\mu j}(Q^2,\Delta t)$ with specific values of i, μ and j. Thus, we can get a similar parametrization for the form factors,

$$F_i(Q^2,\Delta t) \approx F_i(Q^2) + e^{-\delta m \Delta t}, \tag{12}$$

where F_i refers to M_1 or E_2. Note that Q^2 is related to $\vec{p}$ by $Q^2 = 2m_{\eta_1}E_{J/\psi}(\vec{p}) - m^2_{J/\psi} - m^2_{\eta_1}$ here. Since $\Gamma^{(3)}_{i\mu j}(\vec{p},\vec{0};t,t')$ is contributed totally by the disconnected quark diagrams, the signal of $\mathcal{M}^{i\mu j}(\vec{p},t'+\Delta t,t')$ becomes very noisy when $\Delta t \gtrsim 10$ and before a clear plateau appears. Therefore, the resulted $M_1(Q^2,\Delta t)$ and $E_2(Q^2,\Delta t)$ have residual time dependence that is absorbed in an additional exponential term in (12). We use this equation as the fitting formula to obtain the value of F_i and the corresponding error is acquired from jackknife resampling. Figure 4 shows the Δt dependency of $M_1(Q^2,\Delta t)$ and $E_2(Q^2,\Delta t)$, whose δm values are listed in Table II.

The fitted parameters, such as $M_1(Q^2)$, $E_2(Q^2)$, and δm are listed in Table II, where one can see that the values of δm at different Q^2 ($\vec{n}^2$) are more or less the same value

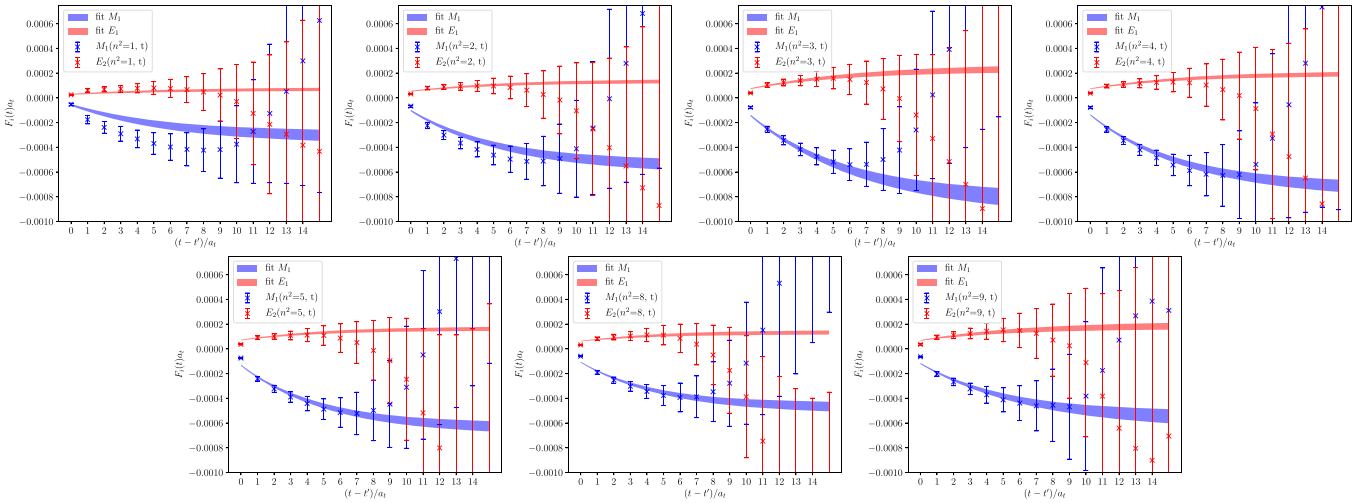

FIG. 4. Multipoles extracted using Eq. (12) with momentum modes $|\vec{n}|^2 = 1, 2, 3, 4, 5, 8, 9$, the shaded curves show the fit ranges and best-fit results.

around 1.2–1.3 GeV. This seems a reasonable value. There are quenched lattice QCD calculations of the masses of the first excited 1^{-+} strangeoniumlike [34] and charmoniumlike states [35], which show that the mass differences of the first excited hybrid states and the ground state hybrids are roughly 1.2–1.3 GeV.

C. On shell form factors and partial decay width

After they are determined at different values of Q^2, $M_1(Q^2)$, and $E_2(Q^2)$ should be interpolated to the on shell values at $Q^2 = 0$, which are required to predict the partial decay width using Eq. (1). If a new Lorentz invariant variable,

$$\begin{aligned}\Omega &= (p \cdot p')^2 - m^2 m'^2 \\ &= \frac{1}{4}[(m+m')^2 + Q^2][(m-m')^2 + Q^2], \end{aligned} \tag{13}$$

is introduced, one can shown that $M_1(Q^2)$ and $E_2(Q^2)$ are proportional to $\sqrt{\Omega}$, namely,

TABLE II. Fitted values of the form factors $M_1(Q^2)$, $E_2(Q^2)$, and δm. The values of χ^2/d.o.f. at different Q^2 are also given.

$\lvert n\rvert^2$	δm/GeV	M_1/GeV	E_2/GeV	χ^2/d.o.f.
1	1.19(33)	−2.22(73)	0.49(20)	0.6
2	1.25(23)	−3.89(74)	0.95(23)	1.0
3	1.08(25)	−6.0(1.3)	1.69(45)	1.0
4	1.21(22)	−5.21(87)	1.38(29)	1.1
5	1.39(24)	−4.49(69)	1.14(24)	1.2
8	1.46(33)	−3.32(63)	0.93(25)	1.0
9	1.16(38)	−4.0(1.1)	1.33(44)	1.0

$$\begin{aligned} M_1(Q^2) &= -\frac{1}{\sqrt{2}}\frac{\sqrt{\Omega}}{mm'}(mG_1(Q^2) + m'G_2(Q^2)), \\ E_2(Q^2) &= \frac{1}{\sqrt{2}}\frac{\sqrt{\Omega}}{mm'}(mG_1(Q^2) - m'G_2(Q^2)), \end{aligned} \tag{14}$$

where the form factors $G_1(Q^2)$ and $G_2(Q^2)$ are defined in Eq. (A1) (for details, see the Appendix). Obviously, $M_1(Q^2)$ and $E_2(Q^2)$ go to zero when $\sqrt{\Omega} \to 0$. This provides an additional constraint for the Q^2 interpolation. When putting $m = m_{J/\psi}$ and $m' = m_{\eta_1}$ back to the above expressions, we have $\sqrt{\Omega(Q^2)} = m_{\eta_1}|\vec{q}|$ in the rest frame of η_1. Therefore, it is convenient to introduce a dimensionless function of Q^2,

$$v(Q^2) \equiv \sqrt{\Omega(Q^2)}/(m_{J/\psi}m_{\eta_1}) = |\vec{q}|/m_{J/\psi}, \tag{15}$$

whose maximum value is $v_{\max}(Q^2) \approx 0.49$ for the momentum $\vec{q}$ involved in this study. Note that the form factors $G_i(Q^2)$ have no singularities when $Q^2 > -m^2_{J/\psi}$. They can be expressed as polynomials of Q^2, and certainly polynomials of $v^2(Q^2)$,

$$G_i(Q^2) = \alpha_i + \beta_i v^2(Q^2) + \delta_i v^4(Q^2) + O(v^6(Q^2)), \tag{16}$$

where the terms up to $\mathcal{O}(v^4(Q^2))$ are kept, since our kinematic configuration that η_1 is at rest and J/ψ moves with a momentum $\vec{q}$, we have a dimensionless quantity, the velocity of J/ψ, $v(Q^2) = \sqrt{\Omega}/(m_{\eta_1}m_{J/\psi}) = |\vec{q}|/m_{J/\psi} < 0.494$ for the values of $\vec{q}$ involved, and $v^6_{\max}(Q^2) \sim 1.4\%$ is already much smaller than our statistical errors. Finally, using Eq. (14), we have the interpolation functions for M_1 and E_2,

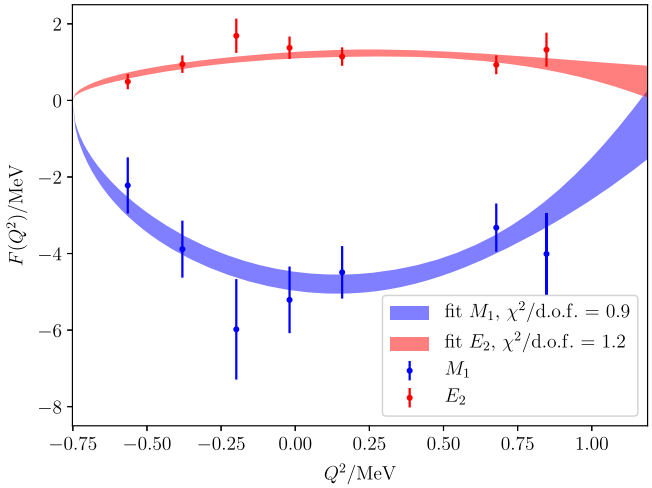

FIG. 5. Form factors $M_1(Q^2)$ and $E_2(Q^2)$ are plotted with respect to Q^2 as data points. The shaded curve illustrates the interpolation using Eq. (17).

$$F_i(Q^2) = v(Q^2)(a_i + b_i v^2(Q^2) + c_i v^4(Q^2)), \quad (17)$$

with the constraint $F_i(Q^2) = 0$ at $v(Q^2) = |\vec{q}|/m_{J/\psi} = 0$ in the rest frame of η_1, as suggested by Ref. [36]. Figure 5 shows the Q^2 dependence of $M_1(Q^2)$ and $E_2(Q^2)$ in the region where we are working. The interpolation using Eq. (17) is also illustrated as a shaded band in Fig. 5 with the best-fit parameters (the width of the band shows the interpolation error). Thus, we get

$$M_1(0) = -4.73(74)\ \text{MeV}$$
$$E_2(0) = 1.18(22)\ \text{MeV}. \quad (18)$$

Putting these values into Eq. (1), the partial width is predicted to be

$$\Gamma(J/\psi \to \gamma\eta_1) = 2.04(61)\ \text{eV} \quad (19)$$

[using the η_1 mass $m_{\eta_1} = 2.230(39)$ GeV]. Note that the form factors in Eq. (18) are obtained by assuming η_1 to be a stable particle, while it must be a resonance in principle. For a resonance R of parameters (m_R, Γ_R), a more systematic approach to derive the form factor $f_R(Q^2)$ from lattice QCD has been proposed in Refs. [37–42], where the finite volume correction are thoroughly discussed for the $1 + \mathcal{J} \to 2$ type transitions with $\mathcal{J}$ being a local current, especially for the case that a resonance can appear in the final two hadron system. However, this approach is unfeasible yet for the processes $J/\psi \to \gamma +$ lighthadron(s) that take place solely through quark annihilation diagrams, because the low precision of $\Gamma^{(3)}_{ij\mu}$ cannot afford that sophisticated treatment. Fortunately, some examples [37,41,42] indicate that the finite volume correction to the form factors of a narrow resonance R is $\mathcal{O}(\Gamma_R/m_R)$, when R is treated as a stable particle. If $\Gamma_{\eta_1}/m_{\eta_1}$ in the $N_f = 2$ case is similar to or even smaller than that of $\eta_1(1855)$, the form factors in Eq. (18) may be taken as approximations for those of the resonant η_1 with regard to their large statistical uncertainties of roughly 15%–20%.

III. DISCUSSION

Although obtained for $N_f = 2$, the form factors in Eq. (18) can be applied to the discussion of the physical SU(3) case. In J/ψ radiative decays, the final state light hadron (η_1 here) is produced by the gluons from the $c\bar{c}$ annihilation, and thereby must be a flavor singlet [isoscalar for $N_f = 2$ and SU(3) singlet for $N_f = 3$]. If the flavor wave function of the light hadron is properly normalized, the underlying gluonic dynamics is usually independent of N_f except for the $U_A(1)$ anomaly relevant interaction. In this sense, the form factors in Eq. (18) can be good approximations of the SU(3) flavor singlet $\eta_1^{(1)}$ up to a kinematic factor owing to the mass mismatch (see below). Due to the flavor SU(3) breaking, there should be two isoscalar mass eigenstates (denoted by $\eta_1^{(l)}$ for the lighter one and $\eta_1^{(h)}$ for the heavier one), which are the admixtures of the singlet $\eta_1^{(1)}$ and the $I = 0$ octet $\eta_1^{(8)}$ through a mixing angle θ, namely,

$$\begin{pmatrix} |\eta_1^{(l)}\rangle \\ |\eta_1^{(h)}\rangle \end{pmatrix} = \begin{pmatrix} \cos\theta & -\sin\theta \\ \sin\theta & \cos\theta \end{pmatrix} \begin{pmatrix} |\eta_1^{(8)}\rangle \\ |\eta_1^{(1)}\rangle \end{pmatrix}. \quad (20)$$

On the other hand, the masses of $\eta_1^{(l,h)}$ can be different from m_{η_1}. In this study, we should consider the correction factor due to the mass mismatch. According to Eq. (14), one has

$$M_1^2(0) + E_2^2(0) = |\vec{q}|^2 \frac{m_{J/\psi}^2}{m_{\eta_1}^2}\left(G_1^2(0) + \frac{m_{\eta_1}^2}{m_{J/\psi}^2} G_2^2(0)\right). \quad (21)$$

Since the form factors $G_i(Q^2)$ are functions of Q^2 and are regular around $Q^2 = 0$, it is expected the form factors $G_i(0)$ for $i = 1, 2$ are insensitive to m_{η_1} in the range $m_{\eta_1} \sim 2$ GeV. For the case of this study, $G_1^2(0)$ is a few times larger than $G_2^2(0)$, such that from Eq. (1), the m_{η_1} dependence is approximately $\Gamma \propto |\vec{q}|^3/m_{\eta_1}^2$. Thus, one has the following partial widths:

$$\Gamma(J/\psi \to \gamma\eta_1^{(l)}) = \chi^{(l)}\Gamma(J/\psi \to \gamma\eta_1)\sin^2\theta$$
$$\Gamma(J/\psi \to \gamma\eta_1^{(h)}) = \chi^{(h)}\Gamma(J/\psi \to \gamma\eta_1)\cos^2\theta, \quad (22)$$

where $\chi^{(x)} = \frac{m_{\eta_1}^2 |\vec{p}_\gamma(\eta_1^{(x)})|^3}{m_{\eta_1^{(x)}}^2 |\vec{p}_\gamma(\eta_1)|^3}$ is the compensating kinematic factor due to the mass mismatch of η_1 and $\eta_1^{(x)}$.

As for the $\eta\eta'$ decay mode where $\eta_1(1855)$ is observed, since it must be a flavor octet, the flavor SU(3) symmetry implies the decay $\eta_1^{(x)} \to \eta\eta'$ takes place only through its octet component, namely, the decay amplitudes satisfy

$$\begin{aligned}\langle\eta\eta'|H_I|\eta_1^{(l)}\rangle &= \cos\theta\langle\eta\eta'|H_I|\eta^{(8)}\rangle \equiv 2g\cos\theta\vec{\epsilon}\cdot\vec{k}^{(l)}\\ \langle\eta\eta'|H_I|\eta_1^{(h)}\rangle &= \sin\theta\langle\eta\eta'|H_I|\eta^{(8)}\rangle \equiv 2g\sin\theta\vec{\epsilon}\cdot\vec{k}^{(h)},\end{aligned} \quad (23)$$

where g is the effective coupling, $\vec{\epsilon}$ is the polarization vector of $\eta_1^{(x)}$, and $\vec{k}^{(x)}$ is the momentum of $\eta\eta'$ in the $\eta^{(x)}$ decay. Thus, we obtain the ratio,

$$r = \frac{\mathrm{Br}(J/\psi \to \gamma\eta_1^{(l)} \to \gamma\eta\eta')}{\mathrm{Br}(J/\psi \to \gamma\eta_1^{(h)} \to \gamma\eta\eta')} = \frac{\chi^{(l)}|\vec{k}^{(l)}|^3 m^2_{\eta_1^{(h)}}}{\chi^{(h)}|\vec{k}^{(h)}|^3 m^2_{\eta_1^{(l)}}} \frac{\Gamma_{\eta_1^{(h)}}}{\Gamma_{\eta_1^{(l)}}}, \quad (24)$$

which is free from θ but depends solely on the masses and widths of $\eta_1^{(l)}$ and $\eta_1^{(h)}$. If the mass difference of $\eta_1^{(l)}$ and $\eta_1^{(h)}$ is not too large, the kinematic factor in the above equation is $\mathcal{O}(1)$, such that one has $r \sim \mathcal{O}(1)\frac{\Gamma_{\eta_1^{(h)}}}{\Gamma_{\eta_1^{(l)}}}$.

The lattice QCD study in Ref. [12] observes $\eta_1^{(l)}$ and $\eta_1^{(h)}$ of masses roughly 2.16 GeV and 2.33 GeV (at $m_\pi \approx 391$ MeV), respectively. They can be admixtures of the flavor singlet $\eta_1^{(1)}$ and the flavor octet $\eta_1^{(8)}$ through a mixing angle θ,

$$\begin{pmatrix}|\eta_1^{(l)}\rangle\\ |\eta_1^{(h)}\rangle\end{pmatrix} = \begin{pmatrix}\cos\theta & -\sin\theta\\ \sin\theta & \cos\theta\end{pmatrix}\begin{pmatrix}|\eta_1^{(8)}\rangle\\ |\eta_1^{(1)}\rangle\end{pmatrix}, \quad (25)$$

or equivalently, the admixtures of $s\bar{s}$ and $n\bar{n} = (u\bar{u}+d\bar{d})/\sqrt{2}$ through a mixing angle α,

$$\begin{pmatrix}|\eta_1^{(l)}\rangle\\ |\eta_1^{(h)}\rangle\end{pmatrix} = \begin{pmatrix}\cos\alpha & -\sin\alpha\\ \sin\alpha & \cos\alpha\end{pmatrix}\begin{pmatrix}|n\bar{n}\rangle\\ |s\bar{s}\rangle\end{pmatrix}. \quad (26)$$

If the flavor wave functions of $\eta_1^{(1)}$ and $\eta_1^{(8)}$ are defined as

$$\begin{aligned}|\eta_1^{(1)}\rangle &= \frac{1}{\sqrt{3}}(|u\bar{u}\rangle + |d\bar{d}\rangle + |s\bar{s}\rangle)\\ |\eta_1^{(8)}\rangle &= \frac{1}{\sqrt{6}}(|u\bar{u}\rangle + |d\bar{d}\rangle - 2|s\bar{s}\rangle),\end{aligned} \quad (27)$$

one can easily show that θ is related to α by $\theta = \alpha - 54.7°$. This convention for the mixing angle α is the same as that in Ref. [12] where α is determined to be roughly $\alpha = 22.7(2.1)°$ (averaged over the values on the three lattices involved), such that one has $\theta \approx -32.0(2.1)°$. This indicates a large mixing of $\eta_1^{(8)}$ and $\eta_1^{(1)}$. Using Eq. (22), the J/ψ total width $\Gamma_{\mathrm{tot}} = 92.6(1.7)$ keV [43] and the observed branching fraction $\mathrm{Br}(J/\psi \to \gamma\eta_1(1855) \to \gamma\eta\eta') = (2.70 \pm 0.41^{+0.16}_{-0.35}) \times 10^{-6}$ [14], we get

$$\begin{aligned}\Gamma(J/\psi \to \gamma\eta_1(1855)) &= (2.0 \pm 0.7)\ \mathrm{eV}\\ \mathrm{Br}(J/\psi \to \gamma\eta_1(1855)) &= (2.1 \pm 0.7) \times 10^{-5}\\ \mathrm{Br}(\eta_1(1855) \to \eta\eta') &= (13 \pm 5)\%\end{aligned} \quad (28)$$

if $\eta_1(1855)$ is assigned to be $\eta_1^{(l)}$, and

$$\begin{aligned}\Gamma(J/\psi \to \gamma\eta_1(1855)) &= (5.0 \pm 1.6)\ \mathrm{eV}\\ \mathrm{Br}(J/\psi \to \gamma\eta_1(1855)) &= (5.4 \pm 1.8) \times 10^{-5}\\ \mathrm{Br}(\eta_1(1855) \to \eta\eta') &= (5.0 \pm 1.9)\%\end{aligned} \quad (29)$$

if $\eta_1(1855)$ is assigned to be $\eta_1^{(h)}$.

Obviously, the existence of the other η_1 state (or not) is crucial for the nature of $\eta_1(1855)$ to be unravelled. We notice BESIII also reports a weak (4.4σ) signal of 1^{-+} component around 2.2 GeV [15]. But its existence needs to be confirmed. On the other hand, if $\eta_1(1855)$ is surely a hybrid state (either $\eta_1^{(l)}$ or $\eta_1^{(h)}$), the results and the discussion imply that the octet $\eta_1^{(8)}$ couples strongly to $\eta\eta'$, namely, the effective coupling in Eq. (23) is roughly $g = 5.0(1.0)$ (note the effective coupling $g_{\rho\pi\pi} \approx 6.0$ for the decay process $\rho \to \pi\pi$). Although there is the possible enhancement by the QCD $U_A(1)$ anomaly [16,17], this is really a large coupling and should be understood when comparing with the significantly small coupling of its isovector partner π_1 to $\eta'\pi$, which is expected by phenomenological studies [44,45] and estimated by lattice QCD calculations [11,13].

IV. SUMMARY

Based on a large gauge ensemble of $N_f = 2$ dynamical quarks at $m_\pi \approx 350$ MeV, we perform the first theoretical calculation of $\Gamma(J/\psi \to \gamma\eta_1)$ where η_1 is the light flavor singlet 1^{-+} hybrid. The related three-point functions are contributed totally from disconnected quark diagrams, which are dealt with using the distillation method. The on shell electromagnetic form factors are determined to be $M_1(0) = -4.73(74)$ MeV and $E_2(0) = 1.18$ MeV, which give $\Gamma(J/\psi \to \gamma\eta_1) = 2.04(61)$ eV for $m_{\eta_1} = 2.23(4)$ GeV. These results are applicable to discuss the production rates of the two mass eigenstates $\eta_1^{(l)}$ and $\eta_1^{(h)}$ in the SU(3) case, if the singlet-octet mixing angle is known. As for $\eta_1(1855)$ observed by BESIII, its hybrid assignment depends strongly on the existence of its mass partner. It should be emphasized that the ratio of the branching fractions $\mathrm{Br}(J/\psi \to \gamma\eta_1^{(l,h)} \to \gamma\eta\eta')$ is inversely proportional to the ratio of the total widths of $\eta_1^{(l,h)}$. This can be used as one of the criteria to identify $\eta^{(l,h)}$

experimentally. If $\eta_1(1855)$ is a hybrid for sure, our results and the mixing angle θ determined in Ref. [12] indicate that the coupling of the octet 1^{-+} hybrid $\eta_1^{(8)}$ to $\eta\eta'$ is very large. This is interesting and worthy of an investigation in depth. Throughout our calculation, η_1 is tentatively viewed as a stable particle. This surely introduce theoretical uncertainties which cannot be accessed in the present stage, but should be explored in future works. Nevertheless, this study provides the first valuable theoretical predictions for this intriguing topic from lattice QCD.

ACKNOWLEDGMENTS

We thank Qiang Zhao for valuable discussions. This work is supported by the National Key Research and Development Program of China (Grant No. 2020YFA0406400), the Strategic Priority Research Program of Chinese Academy of Sciences (Grant No. XDB34030302) and the National Natural Science Foundation of China (NNSFC) under Grants No. 11935017, No. 12075253, No. 12070131001 (CRC 110 by DFG and NNSFC), No. 12175063, No. 12205311, and No. 12293065. The Chroma software system [46] and QUDA library [47,48] are acknowledged. The computations were performed on the HPC clusters at Institute of High Energy Physics (Beijing) and China Spallation Neutron Source (Dongguan), and the ORISE computing environment.

APPENDIX: FORM FACTORS

Since the quantum numbers J^P of η_1 and J/ψ are all 1^-, the transition matrix $\langle\eta_1|j^\mu_{\rm em}|J/\psi\rangle$ is given by the vector-to-vector one $\langle V|j^\mu_{\rm em}|V\rangle$, which can be expanded in terms of form factors by enumerating all possible Lorentz structures,

$$\begin{aligned}&\langle V(p',\epsilon')|j^\mu_{\rm em}|V(p,\epsilon)\rangle\\&= G_1(Q^2)p\cdot\epsilon'^*\epsilon^\mu + G_2(Q^2)p'\cdot\epsilon\epsilon'^{*\mu}\\&\quad+\epsilon\cdot\epsilon'^*[G_3(Q^2)(p^\mu+p'^\mu)+G_4(Q^2)q^\mu]\\&\quad+(p\cdot\epsilon')(p'\cdot\epsilon)[G_5(Q^2)(p^\mu+p'^\mu)+G_6(Q^2)q^\mu].\end{aligned}\tag{A1}$$

$G_4(Q^2)$, $G_6(Q^2)$ can be eliminated and expressed in terms of other form factors using the conservation of current $\langle V|j^\mu_{\rm em}|V\rangle q_\mu = 0$ as

$$\begin{aligned}G_4(Q^2) &= -\frac{m^2-m'^2}{q^2}G_3(Q^2)\\G_6(Q^2) &= -\frac{1}{q^2}[G_2(Q^2)-G_1(Q^2)+G_5(Q^2)(m_i^2-m_f^2)].\end{aligned}\tag{A2}$$

As in Ref. [29] of the main article, it is convenient to expand the helicity amplitudes in terms of *multipoles*. In the frame where the initial state is at rest and the photon goes in the z- direction, the amplitudes are

$$\begin{aligned}\langle V^\mp|j^\mu_{\rm em}|V^0\rangle\epsilon^{\pm,*}_{\gamma,\mu} &= \frac{1}{\sqrt{2}}[M_1(Q^2)+E_2(Q^2)]\\\langle V^0|j^\mu_{\rm em}|V^\pm\rangle\epsilon^{\pm,*}_{\gamma,\mu} &= \frac{1}{\sqrt{2}}[M_1(Q^2)-E_2(Q^2)]\\\langle V^0|j^\mu_{\rm em}|V^0\rangle\epsilon^{0,*}_{\gamma,\mu} &= \frac{1}{\sqrt{3}}C_0(Q^2)-\sqrt{\frac{2}{3}}C_2(Q^2)\\\langle V^\pm|j^\mu_{\rm em}|V^\pm\rangle\epsilon^{0,*}_{\gamma,\mu} &= \frac{1}{\sqrt{3}}C_0(Q^2)+\frac{1}{\sqrt{6}}C_2(Q^2),\end{aligned}\tag{A3}$$

where the superscripts $\mp,\pm,0$ refer the different polarizations of the two vector mesons. On the other hand, these amplitudes can also be expressed in terms of form factors $G_i(Q^2)$ by substituting specific momenta and polarization vectors into Eq. (A1), giving us four equations. By solving these equations, the form factors $G_i(Q^2)$ can be related to multipoles $M_1(Q^2)$, $E_2(Q^2)$, $C_0(Q^2)$, $C_2(Q^2)$ as

$$\begin{aligned}G_1(Q^2) &= \frac{m'}{\sqrt{2\Omega}}(M_1(Q^2)-E_2(Q^2))\\G_2(Q^2) &= \frac{m}{\sqrt{2\Omega}}(M_1(Q^2)+E_2(Q^2))\\G_3(Q^2) &= -\frac{\sqrt{q^2}}{4\sqrt{3\Omega}}(2C_0(Q^2)+\sqrt{2}C_2(Q^2))\\G_5(Q^2) &= \frac{1}{12\sqrt{2}\Omega^{3/2}}\Big[\sqrt{6q^2}((m-m')^2q^2)C_0(Q^2)+\sqrt{3q^2}((m+m')^2+2mm'-q^2)C_2(Q^2)\\&\quad+3(m'-m)((m'+m)^2-q^2)E_2(Q^2)-3(m'+m)((m'-m)^2-q^2)M_1(Q^2)\Big],\end{aligned}\tag{A4}$$

where $Q^2=-q^2$, and

$$\Omega = (p \cdot p')^2 - m^2 m'^2 = \frac{1}{4}[(m+m')^2 + Q^2][(m-m')^2 + Q^2]. \tag{A5}$$

Note that in our case $m = m_{J/\psi}$ and $m' = m_{\eta_1}$.

[1] D. Alde *et al.* (IHEP-Brussels-Los Alamos-Annecy (LAPP) Collaboration), Evidence for a 1^{-+} exotic meson, Phys. Lett. B **205**, 397 (1988).

[2] G. S. Adams *et al.* (E852 Collaboration), Observation of a New $J^{PC} = 1^{-+}$ Exotic State in the Reaction $\pi^- p \to \pi^+\pi^-\pi^- p$ at 18-GeV/c, Phys. Rev. Lett. **81**, 5760 (1998).

[3] M. Aghasyan *et al.* (COMPASS Collaboration), Light isovector resonances in $\pi^- p \to \pi^-\pi^-\pi^+ p$ at 190 GeV/c, Phys. Rev. D **98**, 092003 (2018).

[4] A. Rodas *et al.* (JPAC Collaboration), Determination of the Pole Position of the Lightest Hybrid Meson Candidate, Phys. Rev. Lett. **122**, 042002 (2019).

[5] Hua-Xing Chen, Wei Chen, Xiang Liu, Yan-Rui Liu, and Shi-Lin Zhu, An updated review of the new hadron states, Rep. Prog. Phys. **86**, 026201 (2023).

[6] P. Lacock, Christopher Michael, P. Boyle, and P. Rowland (UKQCD Collaboration), Hybrid mesons from quenched QCD, Phys. Lett. B **401**, 308 (1997).

[7] Claude W. Bernard *et al.* (MILC Collaboration), Exotic mesons in quenched lattice QCD, Phys. Rev. D **56**, 7039 (1997).

[8] Zhong-Hao Mei and Xiang-Qian Luo, Exotic mesons from quantum chromodynamics with improved gluon and quark actions on the anisotropic lattice, Int. J. Mod. Phys. A **18**, 5713 (2003).

[9] C. Bernard, T. Burch, E. B. Gregory, D. Toussaint, Carleton E. DeTar, J. Osborn, Steven A. Gottlieb, U. M. Heller, and R. Sugar, Lattice calculation of 1^{-+} hybrid mesons with improved Kogut-Susskind fermions, Phys. Rev. D **68**, 074505 (2003).

[10] J. N. Hedditch, W. Kamleh, B. G. Lasscock, D. B. Leinweber, A. G. Williams, and J. M. Zanotti, 1^{-+} exotic meson at light quark masses, Phys. Rev. D **72**, 114507 (2005).

[11] C. McNeile and Christopher Michael (UKQCD Collaboration), Decay width of light quark hybrid meson from the lattice, Phys. Rev. D **73**, 074506 (2006).

[12] Jozef J. Dudek, Robert G. Edwards, Peng Guo, and Christopher E. Thomas (Hadron Spectrum Collaboration), Toward the excited isoscalar meson spectrum from lattice QCD, Phys. Rev. D **88**, 094505 (2013).

[13] Antoni J. Woss, Jozef J. Dudek, Robert G. Edwards, Christopher E. Thomas, and David J. Wilson (Hadron Spectrum Collaboration), Decays of an exotic 1^{-+} hybrid meson resonance in QCD, Phys. Rev. D **103**, 054502 (2021).

[14] M. Ablikim *et al.* (BESIII Collaboration), Observation of an Isoscalar Resonance with Exotic $J^{PC} = 1^{-+}$ Quantum Numbers in $J/\psi \to \gamma\eta\eta'$, Phys. Rev. Lett. **129**, 192002 (2022).

[15] M. Ablikim *et al.* (BESIII Collaboration), Partial wave analysis of $J/\psi \to \gamma\eta\eta'$, Phys. Rev. D **106**, 072012 (2022).

[16] Hua-Xing Chen, Niu Su, and Shi-Lin Zhu, QCD axial anomaly enhances the $\eta\eta'$ decay of the hybrid candidate $\eta_1(1855)$, Chin. Phys. Lett. **39**, 051201 (2022).

[17] Lin Qiu and Qiang Zhao, Towards the establishment of the light $J^{P(C)} = 1^{-(+)}$ hybrid nonet, Chin. Phys. C **46**, 051001 (2022).

[18] Vanamali Shastry, Christian S. Fischer, and Francesco Giacosa, The phenomenology of the exotic hybrid nonet with $\pi_1(1600)$ and $\eta_1(1855)$, Phys. Lett. B **834**, 137478 (2022).

[19] Xiang-Kun Dong, Yong-Hui Lin, and Bing-Song Zou, Interpretation of the $\eta_1(1855)$ as a $K\bar{K}_1(1400) + \text{c.c.}$ molecule, Sci. China Phys. Mech. Astron. **65**, 261011 (2022).

[20] Feng Yang, Hong Qiang Zhu, and Yin Huang, Analysis of the $\eta_1(1855)$ as a $KK_1(1400)$ molecular state, Nucl. Phys. **A1030**, 122571 (2023).

[21] Hua-Xing Chen, Atsushi Hosaka, and Shi-Lin Zhu, $I^G J^{PC} = 0^+1^{-+}$ tetraquark state, Phys. Rev. D **78**, 117502 (2008).

[22] Bing-Dong Wan, Sheng-Qi Zhang, and Cong-Feng Qiao, A possible structure of newly found exotic state $\eta_1(1855)$, Phys. Rev. D **106**, 074003 (2022).

[23] Xiangyu Jiang, Feiyu Chen, Ying Chen, Ming Gong, Ning Li, Zhaofeng Liu, Wei Sun, and Renqiang Zhang, Radiative Decay Width of $J/\psi \to \gamma\eta_{(2)}$ from $N_f = 2$ Lattice QCD, Phys. Rev. Lett. **130**, 061901 (2023).

[24] Long-Cheng Gui, Ying Chen, Gang Li, Chuan Liu, Yu-Bin Liu, Jian-Ping Ma, Yi-Bo Yang, and Jian-Bo Zhang (CLQCD Collaboration), Scalar Glueball in Radiative J/ψ Decay on the Lattice, Phys. Rev. Lett. **110**, 021601 (2013).

[25] Yi-Bo Yang, Long-Cheng Gui, Ying Chen, Chuan Liu, Yu-Bin Liu, Jian-Ping Ma, and Jian-Bo Zhang (CLQCD Collaboration), Lattice Study of Radiative J/ψ Decay to a Tensor Glueball, Phys. Rev. Lett. **111**, 091601 (2013).

[26] Long-Cheng Gui, Jia-Mei Dong, Ying Chen, and Yi-Bo Yang, Study of the pseudoscalar glueball in J/ψ radiative decays, Phys. Rev. D **100**, 054511 (2019).

[27] Michael Peardon, John Bulava, Justin Foley, Colin Morningstar, Jozef Dudek, Robert G. Edwards, Balint Joo, Huey-Wen Lin, David G. Richards, and Keisuke Jimmy Juge (Hadron Spectrum Collaboration), A novel

quark-field creation operator construction for hadronic physics in lattice QCD, Phys. Rev. D **80**, 054506 (2009).
[28] Xiangyu Jiang, Wei Sun, Feiyu Chen, Ying Chen, Ming Gong, Zhaofeng Liu, and Renqiang Zhang, η-glueball mixing from $N_f = 2$ lattice QCD, arXiv:2205.12541.
[29] Guo-Zhan Meng *et al.* (CLQCD Collaboration), Low-energy $D^{*+}\bar{D}_1^0$ scattering and the resonance-like structure $Z^+(4430)$, Phys. Rev. D **80**, 034503 (2009).
[30] Jozef J. Dudek, Robert G. Edwards, and David G. Richards, Radiative transitions in charmonium from lattice QCD, Phys. Rev. D **73**, 074507 (2006).
[31] Jozef J. Dudek, Robert Edwards, and Christopher E. Thomas, Exotic and excited-state radiative transitions in charmonium from lattice QCD, Phys. Rev. D **79**, 094504 (2009).
[32] Christopher E. Thomas, Robert G. Edwards, and Jozef J. Dudek, Helicity operators for mesons in flight on the lattice, Phys. Rev. D **85**, 014507 (2012).
[33] Gunnar S. Bali, Bernhard Lang, Bernhard U. Musch, and Andreas Schäfer, Novel quark smearing for hadrons with high momenta in lattice QCD, Phys. Rev. D **93**, 094515 (2016).
[34] Yunheng Ma, Ying Chen, Ming Gong, and Zhaofeng Liu, Strangeonium-like hybrids on the lattice, Chin. Phys. C **45**, 013112 (2021).
[35] Yunheng Ma, Wei Sun, Ying Chen, Ming Gong, and Zhaofeng Liu, Color halo scenario of charmonium-like hybrids, Chin. Phys. C **45**, 093111 (2021).
[36] Yi-Bo Yang, Ying Chen, Long-Cheng Gui, Chuan Liu, Yu-Bin Liu, Zhaofeng Liu, Jian-Ping Ma, and Jian-Bo Zhang (CLQCD Collaboration), Lattice study on η_{c2} and X(3872), Phys. Rev. D **87**, 014501 (2013).
[37] Raúl A. Briceño and Maxwell T. Hansen, Multichannel $0 \to 2$ and $1 \to 2$ transition amplitudes for arbitrary spin particles in a finite volume, Phys. Rev. D **92**, 074509 (2015).
[38] Raúl A. Briceño, Jozef J. Dudek, Robert G. Edwards, Christian J. Shultz, Christopher E. Thomas, and David J. Wilson, The $\pi\pi \to \pi\gamma^\star$ amplitude and the resonant $\rho \to \pi\gamma^\star$ transition from lattice QCD, Phys. Rev. D **93**, 114508 (2016); **105**, 079902(E) (2022).
[39] Raúl A. Briceño, Jozef J. Dudek, and Ross D. Young, Scattering processes and resonances from lattice QCD, Rev. Mod. Phys. **90**, 025001 (2018).
[40] Constantia Alexandrou, Luka Leskovec, Stefan Meinel, John Negele, Srijit Paul, Marcus Petschlies, Andrew Pochinsky, Gumaro Rendon, and Sergey Syritsyn, $\pi\gamma \to \pi\pi$ transition and the ρ radiative decay width from lattice QCD, Phys. Rev. D **98**, 074502 (2018); **105**, 019902(E) (2022).
[41] Raúl A. Briceño, Jozef J. Dudek, and Luka Leskovec, Constraining $1 + \mathcal{J} \to 2$ coupled-channel amplitudes in finite-volume, Phys. Rev. D **104**, 054509 (2021).
[42] Archana Radhakrishnan, Jozef J. Dudek, and Robert G. Edwards (Hadron Spectrum Collaboration), Radiative decay of the resonant K^* and the $\gamma\mathrm{K} \to \mathrm{K}\pi$ amplitude from lattice QCD, Phys. Rev. D **106**, 114513 (2022).
[43] P. A. Zyla *et al.* (Particle Data Group), Review of particle physics, Prog. Theor. Exp. Phys. **2020**, 083C01 (2020).
[44] Philip R. Page, Why hybrid meson coupling to two S wave mesons is suppressed, Phys. Lett. B **402**, 183 (1997).
[45] Philip R. Page, Eric S. Swanson, and Adam P. Szczepaniak, Hybrid meson decay phenomenology, Phys. Rev. D **59**, 034016 (1999).
[46] Robert G. Edwards and Balint Joo (SciDAC, LHPC, and UKQCD Collaborations), The chroma software system for lattice QCD, Nucl. Phys. B, Proc. Suppl. **140**, 832 (2005).
[47] M. A. Clark, R. Babich, K. Barros, R. C. Brower, and C. Rebbi, Solving lattice QCD systems of equations using mixed precision solvers on GPUs, Comput. Phys. Commun. **181**, 1517 (2010).
[48] R. Babich, M. A. Clark, B. Joo, G. Shi, R. C. Brower, and S. Gottlieb, Scaling lattice QCD beyond 100 GPUs, in *SC11 International Conference for High Performance Computing, Networking, Storage and Analysis* (2011), arXiv:1109.2935.